Analysis and Comparison of Control Strategies for a DFIG-Small Wind Turbine System with High Fluctuating Wind Speed Conditions

by Mochammad Facta

Praise Worthy Prize

International Review of Electrical Engineering (I.R.E.E.), Vol. 12, N. 2
ISSN 1827- 6660 March – April 2017

Analysis and Comparison of Control Strategies for a DFIG-Small Wind Turbine System with High Fluctuating Wind Speed Conditions

Iwan Setiawan[1], Mochammad Facta[1], Ardyono Priyadi[2], Mauridhi Hery Purnomo[2]

Abstract – *The main purposes of this paper are to analyse and to compare power quality, modes of machine operation and robusness under two difference control strategies on DFIG-based wind turbine systems: (1) Rotor speed control strategy (RSCS) and (2) Power control strategy (PCS). Both of these strategies could be utilized to maximize wind-power harvesting.In this work, the feedback control loops are designed by using the same optimum Proportional Integral-based vector control strategy. The major focus in this study is on a small-scale wind turbine that characterized by a small mass moment of inertia. By using simulation studies, it is found that the power dynamicresulted by the two control strategiesunder fluctuating wind conditions arerelatively different: the power generated underthe RSCSis more fluctuate compare to the PCS. Even, for extreme cases where the wind speed changes suddenly, the utilization of the RSCSfor a while could bring the machine enters to the motoring mode.In the motoring mode, instead delivering power to the grid, the stator windings of the DFIG will absorb some power from the grid. From simulation results, it is also found that the RSCSin general is less robust compared to the PCS.* ***Copyright © 2017 Praise Worthy Prize S.r.l. - All rights reserved.***

Keywords*: DFIG, Motoring Mode, Power Control Strategy, Rotor Speed Control Strategy*

Nomenclature

A	Turbine blade swept area
B_{wt}	Wind turbine friction coefficient
B_{gen}	Generator friction coefficient
C_p	Turbine power factor
J_{wt}	Turbine inertia
J_{wt}	Wind turbine moment of inertia (kg m^2)
J_g	Generator moment of inertia (kg m^2)
K	Stiffness coefficient
K_p, T_i	Proportional gain and Time integrator of the
L_s	Stator Inductance (H)
L_M	Mutual Inductance (H)
M_{wt}	Turbine mass (kg)
n	Gear ratio
P_{wind}	Wind power (W)
P_{wt}	Wind turbine power output (W)
P_{wt}^*	Optimal wind turbine power output (W)
P_s	Stator active power (W)
Q_s	Stator reactive power (VAr)
R	Turbine blade radius (m)
R_s	Stator Resistance (ohm)
s	Laplace variable
T_{cl}	Time constant of the closed loop system (s)
T_{wt}	wind turbine torque (N m)
T_e	Electromagnetic torque of the generator (N m)
$u_{d(q)r}$	d-q rotor total control output
u_{pi}	Output of PI controller
v	Wind speed (m/s)
v_{ds},i_{ds}	d-axis component of the stator voltage (V) and current vector (A)
v_{dr},i_{dr}	d-axis component of the rotor voltage (V) and current vector (A)
ρ	Air density (kg/m^3)
ω_{wt}	Turbine rotor rotation speed (rad/s)
ω_{wt}^*	Turbine rotor rotation speed reference (rad/s)
β	Blade pitch angle (degree)
λ	Wind turbine tip speed ratio
λ_{opt}	Optimal wind turbine tip speed ratio
ω_r	Generator rotor rotation speed (rad/s)
ψ_{ds}	d-axis component of the stator flux (V m)
ψ_{qs}	q-axis component of the stator flux (V m)
ψ_{dr}	d-axis component of the rotor flux (V m)
ψ_{qr}	q-axis component of the rotor flux (V m)
ω_{se}	Synchronous frequency (rad/s)
ω_{sl}	Slip frequency (rad/s)
σ	Leakage coefficient

I. Introduction

It is well-known that until now, DFIG-based wind turbines are one of the most popular wind power generation systems worldwide [1]-[3].

The DFIG-wind turbine systems could be categorized as variable-speed wind turbines (VAWTs) where the speed of the turbine rotor could be controlled to get optimized wind energy harvesting. Compared to other wind turbine generation systems, the DFIG-wind turbine system is more superior due to several reasons as follows: (1) Independent control of active and reactive powers, (2) Reduction in power converter losses and (3),

https://doi.org/10.15866/iree.v12i2.11387

Reduction in wind turbines mechanical stresses [4]-[7].

Technically, the DFIG is a wound rotor induction machine in which the three stator windings of the machine are directly connected to a three-phase grid, while the rotor windings are connected to the grid via AC/DC/AC converters. In generating the machine mode, the electrical power always flows from the stator to the grid.

However, the direction of power flow in rotor winding basically depends on the state of the rotor speed: if the rotor runs below the synchronous speed of the machine (sub-synchronous), the rotor will receive power from the grid via the AC/DC/AC converters, and conversely if the rotor runs beyond the synchronous speed of the machine (super-synchronous), then the rotor will deliver power to the grid via the same converters.

To maximize the wind power productionof wind turbine systems, an algorithm well-known as maximum power point tracking (MPPT) is usually utilized as a main strategy to extract wind power [8]-[9]. In this strategy, the rotor of the generator varies to track the maximum power generated by the turbine.

The tracking of maximum power using the MPPT algorithms in practice could be implemented in two different ways: (1) The rotor speed control strategy (RSCS) [10]-[13] and (2) the power control strategy (PCS) [14]-[16]. In the RSCS, the MPPT is indirectly achieved by means of a feedback control of the rotor speed. The rotor speed reference in this strategy is derived from the optimal Tip Speed Ratio (TSR) of the wind turbine. Whereas, in the PCS, the MPPT is directly derived by means of a feedback control of the generator stator power.

The stator power reference in this strategy is derived from the slip and the maximum output mechanical power of the wind turbine. Due to the control strategies different principles, the dynamic of the wind turbine variables in general will also be different depending on the chosen strategy.

There are several works trying to investigate the control strategies of the DFIG-based wind turbine systems. In [17], Dongdong Li, et.al investigated the dynamic of the wind turbine variables under RSCS and PCS. To explore the output variable response in transient state, Dongdong Li used step wind changes. The relatively complete investigation of the control strategies and their influences on performance were studied by Ling, Yu et.al. [18]. In their studies, the power output and dynamic rotor speed as well as the power coefficient resulting from control strategies were investigated.

The main objective of this paper is basically in line with the two last papers, however the study of the wind turbine dynamic done in this paper is relatively more complete. Besides investigating the problems of power quality, efficiency, and stability of the rotor speed, the authors also present control design steps and study the effect of controller parameter changes on control system performances. In this work, the focus is on a small scale DFIG-based wind turbine system.

II. System Model

Fig. 1 shows the topology of a typical DFIG-wind turbine system. Compared to other wind turbine-based power generation systems, the control system of a DFIG-wind turbine is relatively complicated. As shown in Fig. 1, there are two converter systems which are independently controlled: a Rotor side converter (RSC) and a Grid side converter (GSC). The major role of the RSC control system is to control rotor excitation current such that the control objective could be achieved. In many cases, the objective of the control system is to extract the maximum wind power by means of a feedback control of the rotor speed or the stator power. Whereas the GSC control system has the main function to inject the energy surplus at the DC bus capacitor to the grid by means of regulating the voltage of the DC bus at a certain level [19].

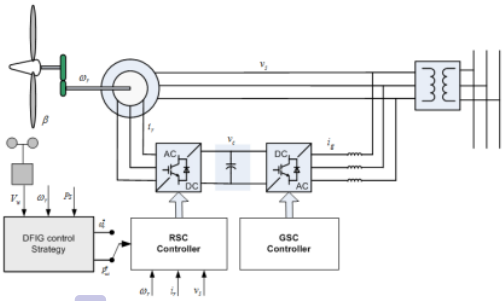

Fig. 1. DFIG-Wind Turbine control system model

The operation mode of these two converters basically depends on the state of the generator rotor speed and will always be opposite: In the sub-synchronous state, the RSC has the role of inverter that converts the DC power of the DC bus capacitor to the AC power of the rotor windings, and at the same time, the GSC has the role of rectifier by converting the AC power of the grid to the DC power of the DC bus capacitor. While at the super-synchronous state, the RSC has the role of rectifier by converting the AC power of the rotor windings to the DC power of the DC bus, and at the same time, the GSC has the role of inverter by converting the DC power of the DC bus to AC power of the grid. Due to the inverse operation of these two converters, the configuration of these converters is also well-known as back to back AC/DC/AC converters.

From the control system point of view, the rotor side DFIG-wind turbine system model is composed of several important component and input models: a wind turbine aerodynamic model, a drive train model, a DFIG model,a wind model, and a control system model.

II.1. A Wind Turbine Aerodinamic Model and MPPT DFIG Control Strategies

A Wind turbine is an energy conversion system that converts wind power into mechanical power and

subsequently transforms this mechanical power into electrical power via a generator. The formulation of wind power-P_{wind} (watt) in general is represented by (1):

$$P_{wind} = \frac{1}{2}\rho A v^3 \quad (1)$$

where ρ, A, and v are respectively air density (kg/m^3), turbine blade swept area (m^2), and wind speed (m/s). However, in practice, wind power cannot be always converted into mechanical power, the power absorption by the wind turbine (P_{wt}) depends on the turbine power factor (C_p) which is affected by the turbine design. Eqs. (2) and (3) respectively show the power and its torque generated by the wind turbine:

$$P_{wt} = \frac{1}{2}\rho A C_p v^3 \quad (2)$$

$$T_{wt} = \frac{P_{wt}}{\omega_{wt}} \quad (3)$$

where ω_{wt} is the turbine rotor rotation speed (rad/s). Referring to [20], the power factor of a wind turbine could be approximated by:

$$C_p = 0.73\left(\left(\frac{1}{\lambda - 0.02\beta} - \frac{0.003}{\beta^3 + 1}\right)15 - 0.58\beta - 0.002\beta^{2.14} - 13.2\right) \times e^{-18.4\left(\frac{1}{\lambda-0.02\beta} - \frac{0.003}{\beta^3+1}\right)} \quad (4)$$

In this case, β and λ are respectively the blade pitch angle (degree) and the wind turbine tip speed ratio-TSR which is defined as:

$$\lambda = \frac{R\omega_{wt}}{v} \quad (5)$$

where R is the turbine blade radius (m). By using (4), the relation between $C_p$with TSR for R=2.5 and several values of β could be shown in Fig. 2.

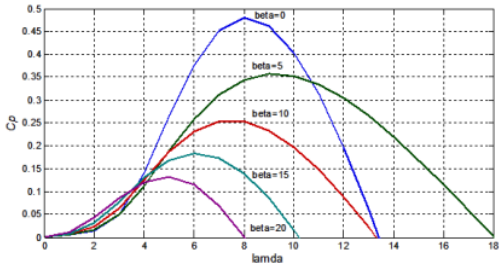

Fig. 2. The plot of C_p vs TSR for several value of β

The important point that can be derived from Fig. 2 is that, for a certain value of β, there is always a maximum point of C_p related to the optimum TSR λ_{opt}. By using it, the maximum wind power could be practically extracted by means of controlling the turbine rotor speed such that an optimum TSR is achieved at any time. This technique is also known as the RSCS. To gain this optimum TSR, the rotor speed reference (ω_{wt}^*) could be directly derived from (5):

$$\omega_{wt}^* = \frac{\lambda_{opt} v}{R} \quad (6)$$

Besides the RSCS, the MPPT could also be achieved by using the PCS. In this strategy, the output power of the wind turbine is directly controlled so that the optimum TSR is achieved at any time. In this control strategy, the power reference could be derived from (2). For the optimum TSR, the arbitrary value of wind speed basically relates to certain turbine rotor speed, so by considering the TSR formulation, the active power reference could be represented as shown in (7):

$$P_{wt}^* = K_{opt}{\omega_{wt}}^3 \quad (7)$$

where:

$$K_{opt} = \left(\frac{1}{2}\frac{\rho A R^3 C_{p\_max}}{{\lambda_{opt}}^3}\right)$$

Fig. 3(a) and Fig. 3(b) respectively show the mechanical turbine power (P_{wt}) and the torque plots versus the turbine rotor rotation speed for several wind speeds along with their references.

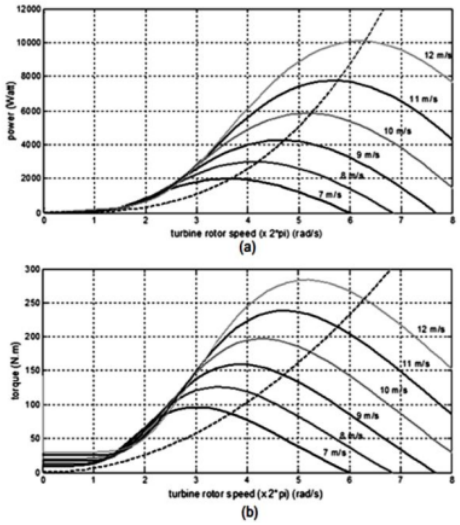

Figs. 3. The dashed line show (a) the power reference and (b) the torque reference in the MPPT strategy (with R=2.5 m)

II.2. Mechanical Drive Train Model

The major purpose of a drive train system in the wind

turbine system is to transmit mechanical power from a low speed wind turbine to a relatively high speed generator. The interconnection of a drive train system could be modeled as shown in Fig. 4 [20]. B_{wt}, B_{gen}, and K respectively are a wind turbine friction coefficient, a generator friction coefficient and a stiffness coefficient. However due to the size of the wind turbine under this study is relatively small, then for control design simplification, the frictions in the system are ignored and it is also assumed that the shaft is very rigid. Therefore with these assumptions, the dynamic model of the mechanical drive train could be represented as one-lumped mass model that could be mathematically represented by (8):

$$\left(\frac{J_{wt}}{n^2}+J_g\right)\frac{d\omega_r}{dt}=T_e-\frac{T_{wt}}{n} \tag{8}$$

where J_{wt}, J_g, n are respectively the wind turbine moment of inertia (kg m^2), the generator moment of inertia (kg m^2) and the gear ratio. Whereas ω_r and T_e are respectively the generator rotor rotation speed (rad/s) and electromagnetic torque of the generator (Nm). By referring to [21], the turbine mass and the turbine inertia could be calculated by using these relations:

$$M_{wt}=1.6R^{2.3} \tag{9}$$

$$J_{wt}=0.212M_{wt}R^2 \tag{10}$$

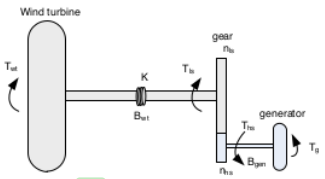

Fig. 4. Mechanical model of the wind turbine and the generator

II.3. DFIG and Grid Mathematical Model

In the synchronous reference frame, the dynamic of the DFIG could be represented as follows [22]:

$$v_{ds}=R_s i_{ds}+\frac{d}{dt}(\psi_{ds})-\omega_{se}\psi_{qs} \tag{11a}$$

$$v_{qs}=R_s i_{qs}+\frac{d}{dt}(\psi_{qs})+\omega_{se}\psi_{ds} \tag{11b}$$

$$v_{dr}=R_r i_{dr}+\frac{d}{dt}(\psi_{dr})-(\omega_{se}-\omega_r)\psi_{qr} \tag{11c}$$

$$v_{qr}=R_r i_{qr}+\frac{d}{dt}(\psi_{qr})+(\omega_{se}-\omega_r)\psi_{dr} \tag{11d}$$

whereas the relations of the currents and flux linkages are:

$$\psi_{ds}=L_s i_{ds}+L_m i_{dr} \tag{12a}$$

$$\psi_{qs}=L_s i_{qs}+L_m i_{qr} \tag{12b}$$

$$\psi_{dr}=L_r i_{dr}+L_m i_{ds} \tag{12c}$$

$$\psi_{qr}=L_r i_{qr}+L_m i_{qs} \tag{12d}$$

In DFIG systems, the electromagnetic torque, the stator active and reactive powers are calculated respectively by using (13), (14) and (15) below:

$$T_e=\frac{3}{2}p(\psi_{ds}i_{qs}-\psi_{qs}i_{ds}) \tag{13}$$

$$P_s=\frac{3}{2}(v_{ds}i_{ds}+v_{qs}i_{qs}) \tag{14}$$

$$Q_s=\frac{3}{2}(v_{qs}i_{ds}-v_{ds}i_{qs}) \tag{15}$$

to control the stator power independently. In this control scheme, the stator flux is aligned with the d-axis of the rotating reference frame. By ignoring the stator flux dynamic and using the fact that the stator resistance is quite small, the d-axis stator flux and the q-axis stator current could be respectively simplified by (16) and (17) below:

$$\psi_{ds}=\frac{v_s}{\omega_{se}} \tag{16}$$

$$i_{qs}=-\frac{L_m}{L_s}i_{qr} \tag{17}$$

By substituting the last two equations into (13)-(15), the electromagnetic torque and the stator power of the DFIG could be respectively represented as follows:

$$T_e=-\frac{3}{2}p\frac{L_m}{L_s}\frac{v_s}{\omega_{se}}i_{qr} \tag{18}$$

$$P_s=-\frac{3}{2}\frac{L_m}{L_s}(v_{qs}i_{qr}) \tag{19}$$

$$Q_s=\frac{3}{2}\left(\frac{{v_{qs}}^2}{\omega_{se}L_s}-\frac{v_{qs}L_m}{L_s}i_{dr}\right) \tag{20}$$

From the last three equations, it is shown that the torque and the active stator power could be controlled by manipulation of the rotor q-axis current component while the reactive power could be controlled by a manipulation of the rotor$d$-axis current component so the decoupled control is achieved.

II.4. Wind Model

The wind speed in a certain time range could be

mathematically expressed as composition of average and perturbation due to wind turbulence [23].

Fig. 5 shows the real sample of a very short term wind speed recorded at Nganjuk, in Indonesia, an area that has high-potential wind energy. However, the wind profile used in this study was generated by the computer program.

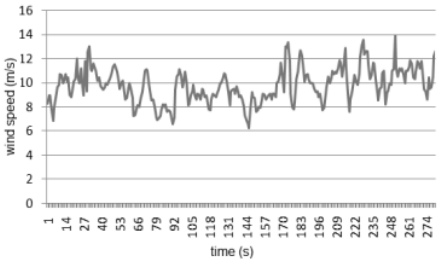

Fig. 5. Real sample of wind speed

III. Control Design

By referring to the DFIG-wind turbine model, the real and reactive power of the system could be respectively controlled by manipulating the *d*-axis and *q*-axis current components of the generator rotor. In DFIG-wind turbine systems, the reference of these current components could be derived from the outer feedback control output of the stator power, as in the power control strategy, or from the outer feedback control output of the rotor speed, as in the rotor speed control strategy.

Therefore, practically there are two control loops which need to be designed: the inner current control loop and the outer power control loop or the rotor speed control.

III.1. Inner Current Control Loop Design

By substituting the rotor dynamics with rotor voltage equations, and doing some simplification steps, the rotor currents dynamic could be derived from:

$$\frac{d}{dt}i_{dr} = -\frac{R_r}{L_r\sigma}i_{dr} + \frac{1}{L_r\sigma}v_{dr} + d_{dr} \tag{21}$$

$$\frac{d}{dt}i_{qr} = -\frac{R_r}{L_r\sigma}i_{qr} + \frac{1}{L_r\sigma}v_{qr} + d_{qr} \tag{22}$$

In this case, σ is well-known as a leakage coefficient, while d_{dr} and d_{qr} could be regarded as disturbances:

$$\sigma = \left[1 - \frac{{L_m}^2}{L_s L_r}\right]$$

$$d_{dr} = \omega_{sl} i_{qr}$$

$$d_{qr} = -\omega_{sl} i_{dr} - \frac{\omega_{sl} L_m}{L_s L_r \delta}\frac{v_s}{\omega_{se}}$$

As shown in (21) and (22), the dynamics of the *d-q* axis current components of the circuit are basically coupled first-order systems. To control the current, the standard PI controller plus the feedforward controller could be utilized as follows:

$$u_{d(q)r} = u_{pi} - d_{d(q)r} \tag{23}$$

where $u_{d(q)r}$ and u_{PI} are respectively the total control output and the PI control output. By substituting (23) to (21) and (22), the dynamics of the *d-q* axis current components could be represented by the transfer function form:

$$H_{d(q)}(s) = \frac{I_{d(q)r}(s)}{u_{d(q)r}(s)} = \frac{1/R_r}{\left(\frac{L_r\sigma}{R_r}\right)s + 1} \tag{24}$$

By utilizing the pole placement technique, the PI control parameters could be easily obtained by using (25):

$$K_i = \frac{R_r}{T_{cl}}, K_P = \frac{L_r\sigma}{T_{cl}} \tag{25}$$

where K_i, K_p and T_{cl} are respectively an integrator gain, a proportional gain and a desired closed loop time constant. The final transfer function of the closed loop system by using the pole placement technique is shown in (26):

$$\frac{I_{d(q)r}(s)}{I^*_{d(q)r}(s)} = \frac{1}{T_{cl}s + 1} \tag{26}$$

III.2. The Outer Loop Control Design

As discussed in Section (2), there are two strategies that could be used to extract the maximum wind turbine power: the PCS and the RSCS. In practice, these two different control strategies could be implemented by using a PI controller where the PI parameter could be tuned by using standard methods.

However, there is one thing that should be carefully considered: The PI mode for the power control strategy and the PI mode for the rotor speed control strategy are different. In this case, the PI mode for the power control strategy is the reverse mode, while the PI mode for the rotor speed control strategy is the direct mode. The determination of the mode of the control strategies could be basically achieved from the analysis of power and torque relation vs rotor speed, as depicted in Fig. 3. From the plots, it could be seen that for a certain wind speed value, the change of real power will have the same direction of the torque change (direct acting) and will have opposite direction with respect to the change of rotor speed (reverse acting). Thus, by considering those facts, the power mode or the torque control is reverse mode, while the mode of the rotor speed control is direct mode, as depicted in Figs. 6.

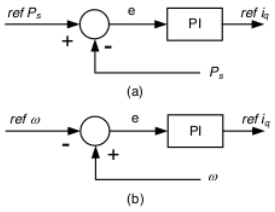

Figs. 6. Controller mode: Reverse mode of the PCS (a) and direct mode of the RSCS (b)

III.2.1. Power Control Loop Design

An easy way to implement PSC is by using the stator power feedback control. By referring to (19) and (26), the transfer function of the real stator power could be rewritten as:

$$\frac{P_s(s)}{I_{qr}^*(s)} = \frac{K}{T_{cl}s + 1} \tag{27}$$

where:

$$K = -\frac{3}{2}\frac{L_m}{L_s}(v_{qs})$$

By using the pole placement technique as done in the current control loop design, the PI controlparameter could be obtained:

$$K_i = \frac{1}{KT_{cl}}, K_P = \frac{1}{K} \tag{28}$$

By using the same technique, it could be proved that the optimal parameter for the reactive power feedback control could also be derived by using (28). Eq. (29) shows the closed loop transfer function of the PCS by using the pole placement technique:

$$\frac{P_s(s)}{p_s^*(s)} = \frac{1}{T_{cl}s + 1} \tag{29}$$

By assuming that the generator is a lossless component, the real stator power reference ($p_s^*(s)$), could be derived from the power balance relation, as shown in (30):

$$P_{wt} = P_s + P_r \tag{30}$$

Considering that $P_r = -sP_s$, then:

$$P_s = \frac{P_{wt}}{1 - s}$$

Therefore, with reference to the optimal power relation in (7), the reference for the real stator power control strategy could be represented as:

$$P_s^* = \frac{K_{opt}}{1 - s}\omega_{wt}{}^3 \tag{31}$$

whereas the reference for the reactive power feedback control is usually set to zero.

III.2.2. Rotor Speed Control Loop Design

With reference to the drive train mechanical model of the wind turbine, the dynamics of the DFIG rotor speed could be basically represented as shown in (32):

$$\frac{d\omega_r}{dt} = \frac{T_e}{J} - \frac{T_{wt}}{nJ} \tag{32}$$

where J is the total moment of the wind turbine and the generator inertia:

$$J = \left(\frac{J_{wt}}{n^2} + J_g\right)$$

By considering (18), then (32) could be rewritten as follows:

$$\frac{d\omega_r}{dt} = \frac{K_e i_{qr}}{J} - \frac{T_{wt}}{nJ} \tag{33}$$

where: $K_e = -\frac{3}{2}p\frac{L_m}{L_s}\frac{v_s}{\omega_{se}}$.

The transfer function ofω_e to I_{qr}^*in this case could be derived by substituting (26) to (33):

$$H(s) = \frac{\omega_e(s)}{I_{qr}^*(s)} = \left(\frac{1}{T_{cl}s + 1}\right)\frac{K_e}{Js} \tag{34}$$

An easy way to get the optimal parameter PI method for the model with the transfer function (34) is by using the symetrical optimum method. By using this technique, the parameter of the PI could be found by:

$$K_P = \frac{J}{aK_eT_{cl}}, K_i = \frac{K_P}{a^2T_{cl}}, \text{where } a = 2,3... \tag{35}$$

IV. Simulation Result and Discussion

To investigate the dynamic of the DFIG-wind turbine under control of the PCS and the RSCS, the complete simulation model based on the component models of the DFIG-wind turbine system has been built under Matlab/Simulink environment. Fig. 7 shows the complete block diagram of the wind turbine control system under simulation study.

The model parameters of the wind turbine used in the study are presented in the Appendix. In this work, the time sampling and the desired time constant for the current and power control loops are 1ms and 10ms respectively. For those parameters, the optimal control parameters which resulted from the design methods are shown in Table I.

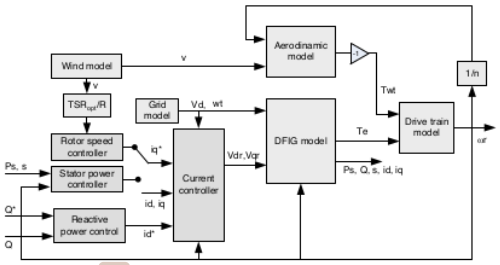

Fig. 7. Block Diagram of the DFIG-wind Turbine model

TABLE I
THE OPTIMAL CONTROL PARAMETERS

Parameter	Current control	Power control	Rotor speed control
K_p	7.197	0.002266	4.26 (a=30)
K_i	650	2.2668	4.73

IV.1. General Performance of the Control Strategies

The performance of the two different control strategies under the same wind speed profile will be evaluated in this Section. Fig. 8 shows the wind speed generated by the computer used in this simulation. For the wind speed profile depicted, the response of the output variables of the DFIG-wind turbine are ploted in Figs. 9 to Fig. 12.

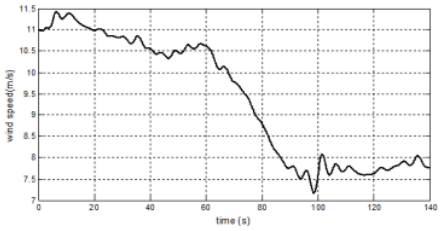

Fig. 8. Random wind profile that used in the simulation

From Fig. 9(a), it is clear that the rotor speed response under PCS and RSCS in general is relatively different. Through a careful observation, it seems obvious that the speed fluctuation that resulted from RSCS is almost the same as the fluctuation of wind speed.

In this case, the more fluctuating the wind speed, the more fluctuating the power generated by the generator too. Whereas, compared to the RSCS, the speed response of the PCSunder the same wind profile looks more dampened.

From Fig. 9(b), it could be seen that for the first 70 seconds simulation time, the relatively high wind speed will make the rotor under both of the control strategies run in super-synchronous state (the slip is negative), while for t>70s where the wind speed starts to slow down, the rotor speed will start to entering the sub-synchronous state and this time the rotor slip will start to be positive.

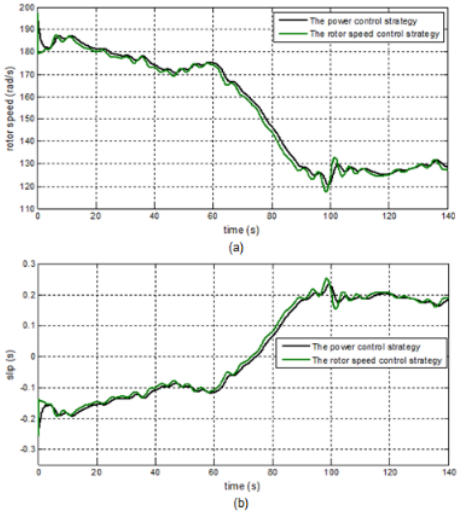

Figs. 9. Response of the rotor speed (a) and the slip of the rotor (b) under two different control strategies

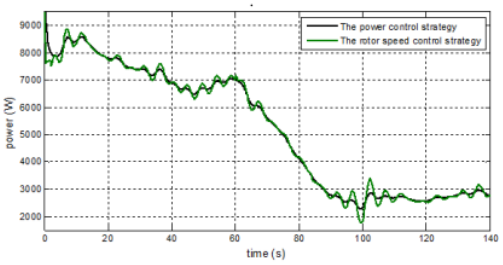

Fig. 10. Response of the total power under two different control strategies

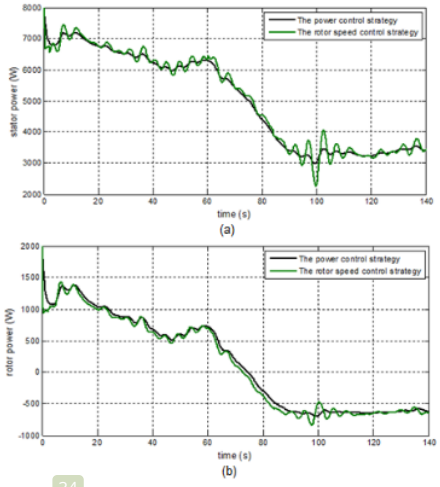

Figs. 11. Response of the stator power (a) and the rotor power (b) under two different control strategies

Fig. 10 shows the DFIG power dynamics for the two control strategies. Almost similar to the response of the rotor speed, the power dynamic resulting from PCS looks more dampened and smooth compared to the power generated by the RSCS. Thus, from the power quality point of view, the PCS is superior compared to the RSCS.

As it has been discussed in Section 2, the total power generated by the DFIG could be basically decomposed in two power components: the stator power and the rotor power. The response of these powers are shown at Fig. 11(a) and Fig. 11(b) respectively. From Fig. 11(a) it is shown that the stator power is always positive, or, in other words, the stator power always flows from the stator to the grid. However, as shown in Fig. 11(b), the direction of the rotor power will basically depend on the rotor slip: in super synchronous condition, the rotor power will be positive, this means that the real power will flow from the rotor to the AC/DC/AC converters, while at the sub-synchronous condition, the power will be negative, this means that the power will flow in the counter direction.

Fig. 12 shows the power coefficient of the wind turbine under two different control strategies. From the plots it is obvious that during power extraction, the power coefficient under the PCSalwaysfluctuates around the optimal value, whereas the power coefficient under the RSCSis almost settled at the optimal value. So from the MPPT point of view, the PCS is less efficient compared to the RSCS.

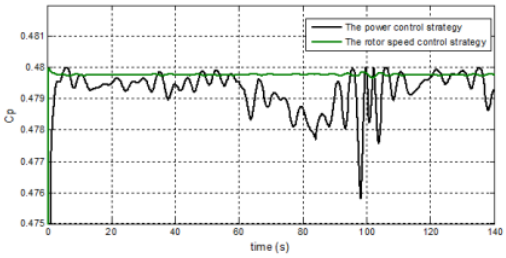

Fig. 12. Power coefficients of the wind turbine under two different control strategies

IV.2. Transient Characteristic: a Deeper Analysis

In this subsection, the transient response of the DFIG output variables such as the rotor speed and the output power under PSC and RSCS will be analized more deeply. As could be seen from the previous results, by using the random wind speed, the dynamic of the wind turbine output variables under the different control strategies are not easy to distinguish. Due to the fact that a wind turbine control system is basically a regulator system as well as a tracking system, the changes of the wind speed in this casecould be regarded as a disturbance to the control system. From the control system point of view, the behavior of the output variables will emerge and look apparent if the wind turbine is disturbed by relatively extreme signals such as step signals.

Therefore, to explore the transient dynamic of wind turbine under extreme case, in this subsection, the control strategy was tested by using wind profile (as shown in Fig. 13), although this wind profile is rather unrealistic in nature.

However, the step changes of wind are suitable to explore the transient characteristic that may be not obvious in the random wind speed profile.For the wind speed profile in Fig. 13, the responses of the rotor speed and the stator power output are depicted in Figs. 14.

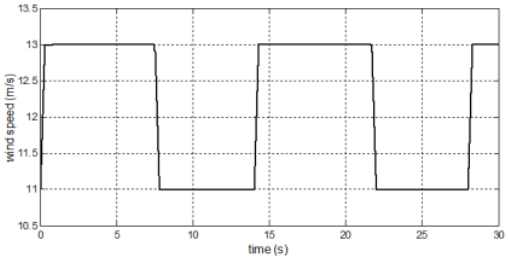

Fig. 13. Almost step changes of the wind speed

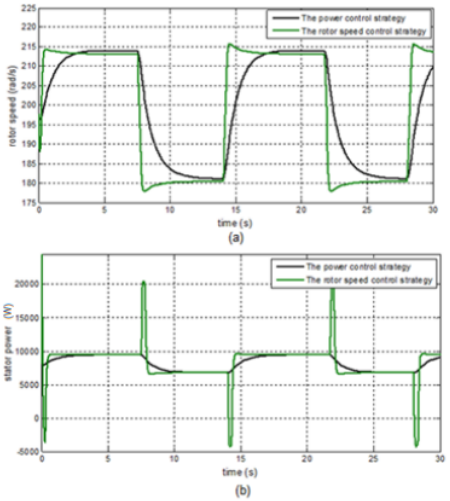

Figs. 14. Response of the rotor speed (a) and the stator power (b) under two different control strategies with wind profile in Fig. 13

From Fig. 14(a) it can be seen that the transient response of the rotor speed under PCS and RSCS are easy to distinguish: in the event of sudden wind changes, the rotor speed under PCS will gradually change.

This is due to two main factors: (1) for every wind change, the turbine inertia (although relatively small) will prevent the rotor speed from being suddenly changed, (2) in the PCS, the reference will also gradually change until a new equilibrium is reached. Whereas the rotor speed under the RSCS will follow the reference changes quickly. The reference changes in the RSCS itself is proportional to the wind speed change, so if the wind

speed suddenly changes, then the rotor speed reference of the RSCS will also change in the same way.

The more interesting result came from the transient state of the stator power output. By looking at Fig. 14(b), the trend of the stator power under the PCS and the RSCS look very different: for sudden changes of the wind speed, the stator power under the PCS will gradually change in the same direction.

This characteristic basically comes from the fact that under the PCS, the stator reference changes for the sudden change of wind speed will be gradual, and in the other side,the transfer function of the model (as discussed in section 3) could be simplified to a first order system.

Whereas, for sudden changes of wind speed, the stator power under the RSCS will also change almost instantaneously and rapidly.

However, as shown from the plot, before the stator power settles to the new equilibrium, the stator power will experience overshoot/undershoot for a while at the opposite direction. This is due to the fact that the mode of the PI controller for the RSCS is a direct mode: for every positive error, the control system will generate a negative control output and vice versa until new equilibrium is reached.

Through a careful observation of Fig. 14(b), it can also be seen that the use of the RSCS for controlling wind turbine systems could make the DFIG enter the motoring mode in the transient state although for a while (generate negative stator power).

IV.3. Control Loop Sensitivity

In this study, the sensitivity of the PSC and RSCS control loops are investigated simply by comparing the transient performance of each control strategy by using two different PI parameters: the optimum PI parameters (Kp_{opt} and Ki_{opt}) and the non-optimum PI parameter ($0.1Kp_{opt}$ and $0.1\ Ki_{opt}$). The wind profile used in this investigation is depicted in Fig. 13.

Fig. 15(a) and Fig. 15(b) respectively show the plots of the slip and stator power under the PCS with these different PI parameters. From the plots, it is shown that the slip and stator power response under PCS are almost the same for the different PI control parameters. In other words, the performance of the PCS is relatively independent from the chosen PI control paramaters.

Whereas, Fig. 16(a) and Fig. 16(b) show the plots of the slip and power stator under the RSCS respectively. From the plots, it is shown that the slip and stator power dynamic under the RSCS for the different PI parameters depicts different characteristics.

In this case, for the non-optimal value of PI parameters, the slip speed will have more overshoot and at the same time the stator power will be more damped for the change of the wind speed compared to the optimal ones.

Thus, the control loop performance of the RSCS is more sensitive to the variation of control parameters compared to PCS.

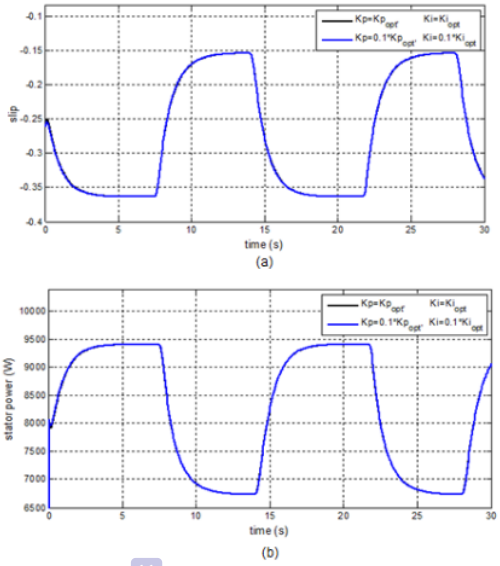

Figs. 15. The slip (a) and the stator power (b) under the power control strategy with different parameters

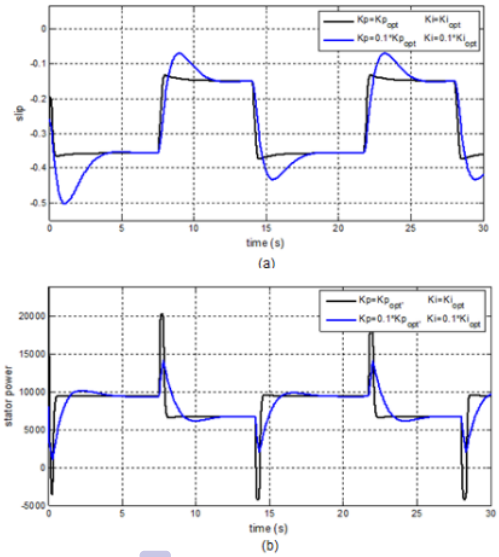

Figs. 16. The slip (a) and the stator power (b) under the rotor speed control strategy with different parameters

V. Conclusion

The analysis and comparison of the performance of DFIG-small scale wind turbines under the PCS and the RSCS have been investigated in this paper. By using the simulation study, it is shown that the output variable dynamics of the DFIG-based wind turbine system under fluctuated wind speed condition strongly depends on the

utilized DFIG-system control strategy. Based on the simulation results, the power coefficient result from the RSCS compared to the PCS during wind tubine operation is almost settled in its optimum value independently from wind speed fluctuation. However, from the the power quality point of view, it is shown that the PCS is superior than the RSCS. In this case, the power dynamics resulted from the PCS is more dampened and smooth compared to the power generated by the RSCS for the same wind fluctuation. From the simulation study, it is also shown that compared to the PCS, the RSCS is very sensitive to the change of the control parameters of the DFIG-wind turbine system.

Appendix

DFIG parameter:
R_r=0.65 ohm, L_r= 67.6e-3 (H), L_m= 63.9e-3 (H), R_s = 0.65 (Ohm), L_s =: 67.6e-3 (H), Pole=2, K_e=5.614, v_s=311, ω_{se}=2×pi×50 rad/s

Wind Turbine parameters:
Blade radius =2.5 (m), Gear ratio=5, J_{gen}=0.0203 (kgm^2), J_{WT}=17.4 (kgm^2), J=0.717(kgm^2)

Acknowledgements

This research was supported by FT Universitas Diponegoro, Indonesia under grant [2932/UN7.3.3/PG/2016].

References

[1] Li, H., and Zhe Chen. "Overview of different wind generator systems and their comparisons." *Renewable Power Generation*, IET 2.2 (2008): 123-138.

[2] Majdoub, Y., Abbou, A., Akherraz, M., El Akhrif, R., Intelligent Backstepping Control of Variable Speed DFIG-Wind Turbine Under Unbalanced Grid Voltage Conditions Using Genetic Algorithm Optimization, (2015) *International Review of Electrical Engineering (IREE),* 10 (6), pp. 716-726.

[3] Setiawan, Iwan, et al. "Adaptive B-spline neural network-based vector control for a grid side converter in wind turbine-DFIG systems." *IEEJ Transactions on Electrical and Electronic Engineering* 10.6 (2015): 674-682.

[4] Anita, BalasubramaniamBabypriya—Rajapalan. "*Modelling, simulation and analysis of doubly fed induction generator for wind turbines*." Journal of Electrical Engineering 60.2 (2009): 79-85.

[5] Abo-Khalil, Ahmed G. "Synchronization of DFIG output voltage to utility grid in wind power system." *Renewable Energy* 44 (2012): 193-198.

[6] Pena, R., J. C. Clare, and G. M. Asher. "Doubly fed induction generator using back-to-back PWM converters and its application to variable-speed wind-energy generation." *IEE Proceedings-Electric Power Applications* 143.3 (1996): 231-241.

[7] Muller, S., M. Deicke, and Rik W. De Doncker. "Doubly fed induction generator systems for wind turbines." *Industry Applications Magazine, IEEE* 8.3 (2002): 26-33.

[8] Luo, Changling, et al. "Strategies to smooth wind power fluctuations of wind turbine generator." *Energy Conversion, IEEE Transactions on* 22.2 (2007): 341-349.

[9] ZENG, Zhiyong, Jing FENG, and Hongfan ZHOU. "MPPT control strategy based on active power reference [J]." *Electric Power Automation Equipment* 6 (2010): 007.

[10] Beltran, Brice, Mohamed El Hachemi Benbouzid, and Tarek Ahmed-Ali. "Second-order sliding mode control of a doubly fed induction generator driven wind turbine." *Energy Conversion, IEEE Transactions on* 27.2 (2012): 261-269.

[11] Mihet-Popa, Lucian, FredeBlaabjerg, and Ion Boldea. "Wind turbine generator modeling and simulation where rotational speed is the controlled variable." *Industry Applications, IEEE Transactions on* 40.1 (2004): 3-10.

[12] Boukhezzar, Boubekeur, and Houria Siguerdidjane. "Nonlinear control with wind estimation of a DFIG variable speed wind turbine for power capture optimization." *Energy Conversion and Management* 50.4 (2009): 885-892.

[13] Khemiri, N., A. Khedher, and M. F. Mimouni. "An adaptive nonlinear backstepping control of DFIG driven by wind turbine." *WSEAS Transactions on Environment and Development* 2 (2012): 60-71.

[14] Wang, Wei, Kang-Zhi Liu, and Tadanao Zanma. "A Gain Scheduled Method for Speed Control of Wind Driven Doubly Fed Induction Generator." *Engineering* 5.01 (2013): 89.

[15] Abdeddaim, S., and A. Betka. "Optimal tracking and robust power control of the DFIG wind turbine." *International Journal of Electrical Power & Energy Systems* 49 (2013): 234-242.

[16] Kerrouche, K., Mezouar, A., Boumediene, L., Belgacem, K., Modeling and Optimum Power Control Based DFIG Wind Energy Conversion System, (2014) *International Review of Electrical Engineering (IREE)*, 9 (1), pp. 174-185.

[17] Li, Dongdong, et al. "The Study of Maximum Power Point Tracking Control for DFIG based on PSCAD." *Journal of International Council on Electrical Engineering* 2.3 (2012): 326-333.

[18] Ling, Yu, Guoxiang Wu, and XuCai. "Comparison of wind turbine efficiency in maximum power extraction of wind turbines with doubly fed induction generator." *Przegląd Elektrotechniczny Electrical Review* 5 (2012).

[19] Setiawan, I., Priyadi, A., Purnomo, M., Control Strategy Based on Associative Memory Networks for a Grid-Side Converter in On-Grid Renewable Generation Systems Under Generalized Unbalanced Grid Voltage Conditions, (2016) *International Review of Electrical Engineering (IREE)*, 11 (2), pp. 171-182.

[20] Fletcher, John, and Jin Yang. Introduction to the doubly-fed induction generator for wind power applications. *INTECH Open Access Publisher*, 2010.

[21] Rodriguez, A. G., A. González Rodríguez, and M. Burgos Payán. "Estimating wind turbines mechanical constants." *Proc. Int. Conf. Renewable Energies and Power Quality (ICREPQ'07)*. 2007.

[22] Luna, Alvaro, et al. "Comparison of power control strategies for DFIG wind turbines." *Industrial Electronics, 2008. IECON 2008. 34th Annual Conference of IEEE*. IEEE, 2008.

[23] Luo, Changling, et al. "Strategies to smooth wind power fluctuations of wind turbine generator." *Energy Conversion, IEEE Transactions on* 22.2 (2007): 341-349.

Authors' information

[1]Department of Electrical Engineering, Universitas Diponegoro, Semarang 50275, Indonesia.
E-mail: iwansetiawan@live.undip.ac.id

[2]Department of Electrical Engineering, Institut Teknologi Sepuluh Nopember, Surabaya 60111, Indonesia.

Iwan Setiawan received the B.Eng and M.Eng degrees from the Engineering Faculty of Gadjah Mada University, Indonesia in 1998 and 2003, respectively. In 2016 he received Doctor degree from Electrical Engineering Dept.of Institut Teknologi Sepuluh Nopember, Indonesia.He is currently anassociate professor atUniversitas Diponegoro, Semarang, Indonesia.
His research interest include control design for power systems and renewable energy.

Mochammad Facta received the B.Eng degree from the Engineering Faculty of Hasanudin University, Indonesia in 1996, in 1999 he received MS degree from Institut Teknologi Sepuluh Nopember, Indonesia. His Ph.D is received from Universiti Teknologi Malaysia in 2012. He is currently anassociate professor atUniversitas Diponegoro, Semarang. His research interests include powersystem and power electronic.

Ardyono Priyadi received the B.Eng degree from the Engineering Faculty of Institut Teknologi Sepuluh Nopember, Indonesia in 1997, in 2008 and 2011, respectively, he received MS and Ph.D degree from Hiroshima University, Japan. He is currently a lectureratInstitut Teknologi Sepuluh Nopember. His research interests include powersystem and stability.

Mauridhi Hery Purnomo received the B.Eng degree from the Engineering Faculty of Institut Teknologi Sepuluh Nopember, Indonesia in 1985, in 1995 and 1998, he received MS and PhD degree from Osaka City University, Japan respectively. He is currently a Professor at Institut Teknologi Sepuluh Nopember. His research interests include power system and intelligent systems.

Analysis and Comparison of Control Strategies for a DFIG-Small Wind Turbine System with High Fluctuating Wind Speed Conditions

ORIGINALITY REPORT

12%	7%	10%	2%
SIMILARITY INDEX	INTERNET SOURCES	PUBLICATIONS	STUDENT PAPERS

PRIMARY SOURCES

1	bura.brunel.ac.uk Internet Source	<1%
2	A.P. Morando. "Dynamic electromechanical model of a high speed train", IEEE Power Engineering Society General Meeting 2004 PES-04, 2004 Publication	<1%
3	Hani Alhamed Aldwaihi, Emmanuel Delaleau. "Maximum power point tracker of a wind generator based on the Flatness-based control", 2011 IEEE Energy Conversion Congress and Exposition, 2011 Publication	<1%
4	Submitted to University of Surrey Roehampton Student Paper	<1%
5	resits.its.ac.id Internet Source	<1%

Submitted to Politeknik Negeri Bandung

6	Student Paper	<1%
7	A. Priyadi, N. Yorino, M. Eghbal, Y. Zoka, Y. Sasaki, H. Yasuda, H. Kakui. "Transient stability assessment as boundary value problem", 2008 IEEE Canada Electric Power Conference, 2008 Publication	<1%
8	Submitted to University of Northumbria at Newcastle Student Paper	<1%
9	es.scribd.com Internet Source	<1%
10	J. Morren, S.W.H. deHaan. "Ridethrough of Wind Turbines with Doubly-Fed Induction Generator During a Voltage Dip", IEEE Transactions on Energy Conversion, 2005 Publication	<1%
11	Larbi Djilali, Edgar N. Sanchez, Mohammed Belkheiri. "Real-time Neural Input–Output Feedback Linearization control of DFIG based wind turbines in presence of grid disturbances", Control Engineering Practice, 2019 Publication	<1%
12	eprints.lib.hokudai.ac.jp Internet Source	<1%

13	kth.diva-portal.org Internet Source	<1 %
14	sites.google.com Internet Source	<1 %
15	www.ijmetmr.com Internet Source	<1 %
16	T. Petru, T. Thiringer. "Modeling of wind turbines for power system studies", IEEE Transactions on Power Systems, 2002 Publication	<1 %
17	Submitted to University of Melbourne Student Paper	<1 %
18	researchinventy.com Internet Source	<1 %
19	www.akamaiuniversity.us Internet Source	<1 %
20	www.ieomsociety.org Internet Source	<1 %
21	actapress.com Internet Source	<1 %
22	www.intechopen.com Internet Source	<1 %
23	Y. Lei, A. Mullane, G. Lightbody, R. Yacamini. "Modeling of the Wind Turbine With a Doubly	<1 %

	Fed Induction Generator for Grid Integration Studies", IEEE Transactions on Energy Conversion, 2006 Publication	
24	etheses.bham.ac.uk Internet Source	<1 %
25	hdl.handle.net Internet Source	<1 %
26	ir.uiowa.edu Internet Source	<1 %
27	scholarcommons.usf.edu Internet Source	<1 %
28	H.G. Beyer, T. Degner, H. Gabler. "Operational behaviour of wind diesel systems incorporating short-term storage: An analysis via simulation calculations", Solar Energy, 1995 Publication	<1 %
29	Shanzhi Li, Haoping Wang, Yang Tian, Abdel Aitouche. "A sliding model control based on intelligent PID control for wind turbine system", 2015 4th International Conference on Systems and Control (ICSC), 2015 Publication	<1 %
30	Wei Wang. "A Gain Scheduled Method for Speed Control of Wind Driven Doubly Fed Induction Generator", Engineering, 2013	<1 %

	Publication	
31	addi.ehu.es Internet Source	<1 %
32	eprints.whiterose.ac.uk Internet Source	<1 %
33	era.ed.ac.uk Internet Source	<1 %
34	new.jee.ro Internet Source	<1 %
35	red.pe.org.pl Internet Source	<1 %
36	Abdou, A. F., A. Abu-Siada, and H. R. Pota. "Effect of intermittent voltage source converter faults on the overall performance of wind energy conversion system", International Journal of Sustainable Energy, 2014. Publication	<1 %
37	Ahmed G. Abo-Khalil. "Synchronization of DFIG output voltage to utility grid in wind power system", Renewable Energy, 2012 Publication	<1 %
38	Ana Fernández-Guillamón, Emilio Gómez-Lázaro, Eduard Muljadi, Ángel Molina-García. "Power systems with high renewable energy sources: A review of inertia and frequency	<1 %

control strategies over time", Renewable and Sustainable Energy Reviews, 2019
Publication

---

39 Binayak Bhandari, Shiva Raj Poudel, Kyung-Tae Lee, Sung-Hoon Ahn. "Mathematical modeling of hybrid renewable energy system: A review on small hydro-solar-wind power generation", International Journal of Precision Engineering and Manufacturing-Green Technology, 2014 <1 %
Publication

---

40 Bowtell, L., and A. Ahfock. "Direct current offset controller for transformerless single-phase photovoltaic grid-connected inverters", IET Renewable Power Generation, 2010. <1 %
Publication

---

41 C. Nichita, D. Luca, B. Dakyo, E. Ceanga. "Large band simulation of the wind speed for real time wind turbine simulators", IEEE Transactions on Energy Conversion, 2002 <1 %
Publication

---

42 C.T. Kiranoudis, N.G. Voros, Z.B. Maroulis. "Wind energy exploitation for reverse osmosis desalination plants", Desalination, 1997 <1 %
Publication

---

43 J.W. Smith, J.A. Taylor, D.L. Brooks, R.C. Dugan. "Interconnection studies for wind <1 %

generation", Rural Electric Power Conference, 2004, 2004
Publication

---

44 K. Halbaoui, D. Boukhetala, F. Boudjema. "Speed Control of Induction Motor Drives Using a New Robust Hybrid Model Reference Adaptive Controller", Journal of Applied Sciences, 2009 <1 %
Publication

---

45 Mohammed El malah, Abdellfattah Ba-razzouk, El Hassane Abdelmounim, Mhamed Madark. "Backstepping Controllers Design for a Grid Connected Wind-Photovoltaic Hybrid Power System", 2020 5th International Conference on Renewable Energies for Developing Countries (REDEC), 2020 <1 %
Publication

---

46 Oscar Barambones. "Robust Wind Speed Estimation and Control of Variable Speed Wind Turbines", Asian Journal of Control, 2018 <1 %
Publication

---

47 Stevanoski, Blagoja, Mile Spiroski, and Mile Joncevski. "Dynamic characteristics of a DFIG wind turbine connected to the transmission power system of Republic of Macedonia", 4th International Conference on Power Engineering Energy and Electrical Drives, 2013. <1 %
Publication

48	Yoonsu Nam, Jeong-gi Kim, Carlo L. Bottasso. "Maximal power extraction strategy in the transition region and its benefit on the AEP (annul energy product)", Journal of Mechanical Science and Technology, 2011 Publication	<1 %
49	biblio.ugent.be Internet Source	<1 %
50	iosrjournals.org Internet Source	<1 %
51	research.sabanciuniv.edu Internet Source	<1 %
52	www.ajer.org Internet Source	<1 %
53	www.praiseworthyprize.org Internet Source	<1 %
54	Fengxiang Wang, Chengwu Lin, Jianguang Zhu, Longya Xu. "A chopping and doubly-fed adjustable speed system without bi-directional converter", Conference Record of the 2002 IEEE Industry Applications Conference. 37th IAS Annual Meeting (Cat. No.02CH37344), 2002 Publication	<1 %
55	Hansen, A.D.. "Fault ride-through capability of DFIG wind turbines", Renewable Energy,	<1 %

200707
Publication

56	K. Belmokhtar, M.L. Doumbia, K. Agbossou. "Novel fuzzy logic based sensorless maximum power point tracking strategy for wind turbine systems driven DFIG (doubly-fed induction generator)", Energy, 2014 Publication	<1 %
57	Maria Auxiliadora Muanis Persechini, Fábio Gonçalves Jota. "Centralized and distributed control architectures under Foundation Fieldbus network", ISA Transactions, 2013 Publication	<1 %
58	Shenglong Yu, Junhao Guo, Tatkei Chau, Tyrone Lucius Fernando, Herbert Iu, Hieu Trinh. "An Unscented Particle Filtering Approach to Decentralized Dynamic State Estimation for DFIG Wind Turbines in Multi-Area Power Systems", IEEE Transactions on Power Systems, 2020 Publication	<1 %
59	Tarek H.M. El Fouly. "A combined electro-mechanical control technique for dynamic voltage regulation of a stand-alone wind turbine generator", International Journal of Global Energy Issues, 2006 Publication	<1 %

60	Ping-Kwan Keung, , Pei Li, H. Banakar, and Boon Teck Ooi. "Kinetic Energy of Wind-Turbine Generators for System Frequency Support", IEEE Transactions on Power Systems, 2009. Publication	<1 %

Exclude quotes	Off	Exclude matches	Off
Exclude bibliography	On		

Analysis and Comparison of Control Strategies for a DFIG-Small Wind Turbine System with High Fluctuating Wind Speed Conditions

GRADEMARK REPORT

FINAL GRADE

/0

GENERAL COMMENTS

Instructor

PAGE 1

PAGE 2

PAGE 3

PAGE 4

PAGE 5

PAGE 6

PAGE 7

PAGE 8

PAGE 9

PAGE 10

PAGE 11